

Surface structure of ferroelectric domains on the triglycine sulfate (010) surface

H. Bluhm and R. Wiesendanger

Institute of Applied Physics and Microstructure Research Center, University of Hamburg, Jungiusstrasse 11, D-20355 Hamburg, Germany

K.-P. Meyer

Max Planck Institute of Microstructure Physics, Weinberg 2, D-06120 Halle (Saale), Germany

(Received 24 July 1995; accepted 2 January 1996)

Scanning force microscopy investigations on the triglycine sulfate (010) surface were carried out employing the method of matched faces. The difference in the etch rate of surfaces of ferroelectric domains with opposite polarity as observed with optical microscopy and scanning electron microscopy could be confirmed. The shape of the etch products on domains with equal polarity on the matching surfaces was found to vary widely. The height and direction of steps at the domain boundaries were measured and discussed with respect to earlier work done by means of transmission electron microscopy. A model which explains the differences in the step heights at the domain boundaries is given under consideration of the shift in the atom positions during ferroelectric polarization reversal. © 1996 American Vacuum Society.

I. INTRODUCTION

Since the discovery of its ferroelectric nature in 1956¹ triglycine sulfate (TGS) is one of the best studied ferroelectric materials. Below the Curie point TGS exhibits antiparallel 180° domains, which are generally rodlike parallel to the **b** axis.^{2,3} The domain structure was observed by transmission electron microscopy (TEM) using decoration technique,^{4,5} scanning electron microscopy (SEM),^{6,7} scanning force microscopy (SFM),⁸ and differential interference microscopy.⁹ For optical microscopy studies the liquid crystal method^{10,11} and the etching method¹²⁻¹⁵ were employed as well. The method of matched faces has already been used for the study of the domain structure of ferroelectric crystals.^{5,9}

When TGS is kept under ambient conditions a thin water film is formed at the crystal faces.¹⁶ Due to its reactivity with polar liquids (as, e.g., water) the surface of TGS is etched. It has been found that the surfaces of domains with opposite sign of polarization show different etch rates.¹⁷ The resulting variance of the surface roughness causes domain contrast in optical microscopy studies and has also been used for the denomination of the domain polarity in SFM and friction force microscopy (FFM) studies.^{8,18}

Here, we report on SFM investigations on matched cleavage faces on TGS. It will be shown that the fine structure of the etch pattern can vary widely for domains of equal polarity. Additionally, the change of the relative position of the cleavage plane in the TGS unit cell at domain boundaries is compared with results obtained by TEM.¹⁹ Small deviations in the predicted step height are explained under consideration of the shifted atom positions for domains of opposite polarity.

II. EXPERIMENT

The TGS single crystals were grown from aqueous solution at a constant temperature above the Curie point

($T_c = 49^\circ\text{C}$). The lattice constants of the monoclinic unit cell are $\mathbf{a} = 0.15 \text{ \AA}$, $\mathbf{b} = 12.69 \text{ \AA}$, $\mathbf{c} = 5.73 \text{ \AA}$, and $\beta = 105^\circ 40'$.²⁰

The crystal structure is given in Fig. 1. The atom positions were taken from Hoshino *et al.*²¹ and transformed to the crystal axes used in Ref. 20. The transformation matrix is given in Ref. 22. The structure consists of four different layers (depicted by A, A', B, and B' in Fig. 1) which have either a different chemical consistence or a different orientation. Both layers A and A' contain SO₄-glycine 1 (G1) molecules, whereas B and B' are built up from glycine 2 (G2)-glycine 3 (G3) molecules (the abbreviations and names for the glycine molecules are used as in Ref. 21). Neighboring layers have an average distance of $\mathbf{b}/4$, closest layers of identical chemical composition are separated by $\mathbf{b}/2$.

The principle of the method of matched faces is sketched in Fig. 2. TGS can easily be cleaved parallel to the (010) plane. For each measurement, a (010) oriented TGS plate with a thickness of about 2 mm was cleaved in its middle. Afterwards, the two freshly generated surfaces (denoted by "I" and "II" in the following) were inspected by optical microscopy in order to find a characteristic surface spot for the subsequent force microscopy measurements.

The SFM investigations were carried out immediately after the sample preparation. A commercially available scanning force microscope²³ was used. The instrument was operated in contact mode under ambient conditions with loadings of about 30 nN. The V-shaped silicon nitride cantilevers with integrated pyramidal tips²³ had force constants of about 0.06 N/m.

The values for the step heights given in this article are mean values determined from height histograms and averaged from measurements at different surface spots. The error in the z values is $\pm 0.05 \text{ nm}$.

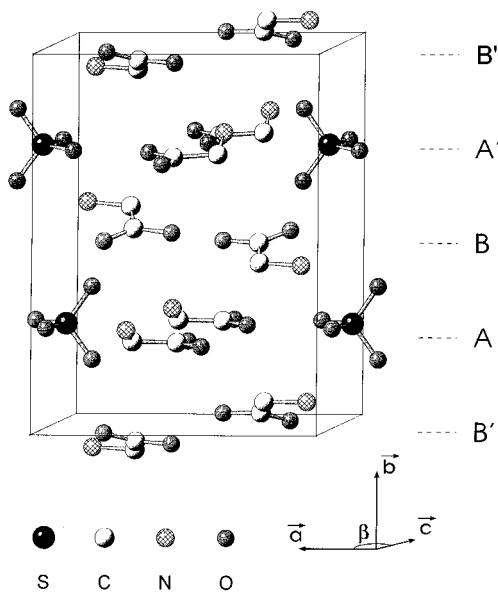


FIG. 1. Crystal structure of a TGS unit cell. TGS can be considered to consist of layers stacked along the **b** axis. The hydrogen atoms are neglected.

III. RESULTS AND DISCUSSIONS

Figure 3(a) shows a $10 \times 10 \mu\text{m}^2$ SFM micrograph of the freshly cleaved surface I. A typical zig-zag cleavage step structure is dominant. The double steps have heights of one unit cell in the **b** direction.

The image is divided into two areas which are separated by a step with height 0.26 nm [see arrows in Fig. 3(a)]. Whereas on the right-hand side the terraces are perfectly smooth with only a few small holes, the left-hand side comprises many round islands. Both islands and holes are separated by steps of height $\mathbf{b}/2$ (0.65 nm) from the surrounding terrace.

From previous investigations it is known that the domains with an opposite sign of polarization show a different etching behavior.²⁴ Positive domains are etched stronger than negative ones. Considering the differences in the etching behav-

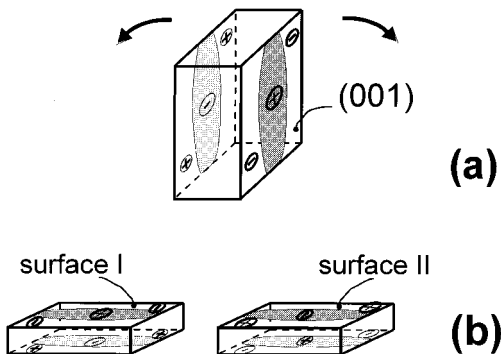


FIG. 2. Principle of the method of matched faces. (a) Sample before cleavage. The two (001) faces show a reversed domain structure. (b) The two freshly generated surfaces I and II show an opposite domain structure.

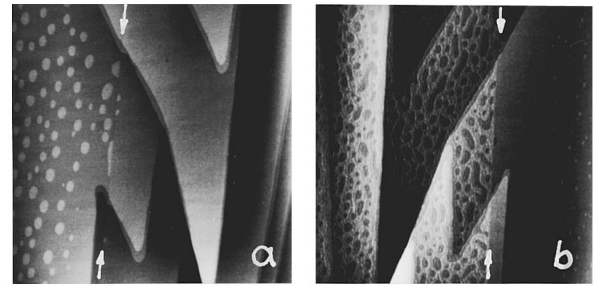


FIG. 3. (a) $10 \times 10 \mu\text{m}^2$ topographical image of the (010) surface of sample I. The position of a domain boundary is marked by arrows. (b) $10 \times 10 \mu\text{m}^2$ topographical image of the surface spot on sample II which matches (a). The domain boundary is marked by arrows.

ior, the left-hand side in Fig. 3(a) is the surface of a positive domain, whereas the right-hand side is the surface of a negative domain, respectively.

Figure 3(b) shows the corresponding area on sample II. The cleavage structure matches perfectly with that of sample I. Two domains can be distinguished from their different etching behavior. The area on the left-hand side from the domain boundary is much stronger etched and reveals a lot of irregularly shaped holes, while the right-hand side is comparatively smooth with few small islands. Therefore, it is concluded that the left-hand side in Fig. 3(b) is the surface of a positive domain, whereas the right-hand side is the surface of a negative domain. This is in agreement with the fact that the region which is the surface of a positive domain at surface I [Fig. 3(a)] should be the surface of a negative domain at surface II [Fig. 3(b)] and vice versa (see Fig. 2).

The domain boundary on surface II appears as a step with 0.37 nm height. However, this step is not matching with the step at the domain boundary at surface I, i.e., the step has not the correct direction in order to fit with the corresponding step. This is illustrated in Fig. 4, which gives a sketch of the observed etch behavior and the direction of the steps at the domain boundaries of the corresponding surface areas.

The steps occurring at the domain boundaries on the surfaces I and II are in agreement with an earlier work done by means of TEM.¹⁹ The experiment utilizing a combination of low-angle shadowing technique and decoration technique revealed steps of about $\mathbf{b}/4$ height between neighboring domains of opposite sign. Considering the crystal structure of TGS, the author of this work argued that there is a change in the chemical composition of the topmost surface layer for domains with opposite sign. It was concluded that the surface of a negative domain always contains G2–G3 molecules (layer B or B' in Fig. 1, respectively), while the surface of a positive domain consists of G1 and SO_4 molecules (layer A or A').

Additionally, it was found in the TEM measurements¹⁹ that the surface of the positive domains is merely raised by the step of $\mathbf{b}/4$ above the surface of the negative domains. In our measurements this is only valid for Fig. 3(b) (surface II). Surface I exhibits the opposite behavior: the negative domain is raised above the positive domain thus causing a mismatch

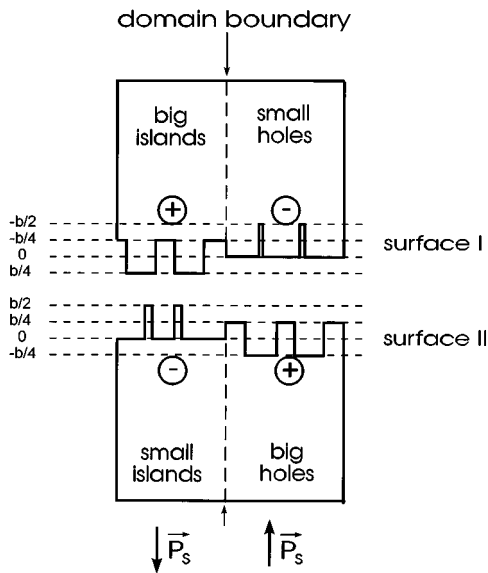


FIG. 4. Schematic drawing of the surface structure of the opposite cleavage faces. The step heights are given with respect to the surface of the negative domains. Note the $b/4$ steps at the domain boundaries, which do not match. The etch fine structure is different between domains of opposite polarity as well as between domains with equal polarity on opposite cleavage faces.

of the corresponding surfaces at the domain boundary (see Fig. 4).

The different etching behavior of positive and negative domains is discussed in Ref. 17. Etching experiments of TGS in different solutions revealed the positive glycinium ions to play the major role in surface etching. Since the diffusion rate of the positive glycinium ions near the positive end of a domain is larger than near the negative end, the positive domains are etched faster than the negative ones. It is remarkable that the strong etching of the positive domain shows up at one surface as formation of round islands (surface I), whereas at the other surface (surface II) the etching results in irregularly shaped holes.

A detailed survey over etching of crystals is given in Ref. 25. The formation of etch holes on crystal surfaces as observed on the positive domain of sample II is a well-known phenomenon (see Ref. 25, and references therein). For the occurrence of the round islands on the positive domain of sample I several explanations can be considered, such as the formation of so-called "spurious" etch pits formed as residuals of etch hole formation,²⁶ "true" etch pit generation (see, e.g. Refs. 26–31), dislocation etching as already observed in ferroelectric materials,^{32–34} and recrystallization as argued in Ref. 8.

However, there is strong evidence that a recrystallization process is the proper model which explains the existence of the round islands. Figure 5(a) shows the surface of a positive domain exhibiting cleavage steps and etch holes. After scanning the tip for about 10 min over an area of $100 \times 100 \text{ nm}^2$, an island was formed right under the scanned tip. The terrace underneath is etched back at the surface step close to the scanned area. These observations, which are reproducible, point to a tip-induced etching and recrystallization at the

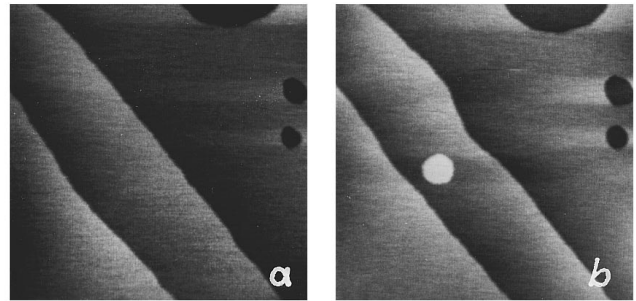


FIG. 5. (a) $1 \times 1 \mu\text{m}^2$ topographical image of the surface of a positive domain. (b) SFM image of the same surface spot after the tip was scanned over an area of $100 \times 100 \text{ nm}^2$ for about 10 min. A new island was grown under the tip. The shape of the lower step close to the new island has changed. This points to a tip-induced etching and recrystallization of TGS.

surface. The presence of the AFM tip is changing the chemical potential at the tip-sample contact area thus promoting the recrystallization of material from the saturated solution at the surface.

This observation leads to a possible explanation for the mismatch of samples I and II at the domain boundaries as described above (see Fig. 4): On surface I a complete monolayer with a thickness of $b/2$ on the positive domain is dissolved. Subsequently, recrystallization from the saturated solution takes place on the positive domain leading to a topography as observed in Fig. 3(a). According to this suggestion, samples I and II would show perfect fit also at the domain boundaries in the moment of cleavage.

The different step heights measured at the domain boundaries on samples I (0.26 nm) and II (0.37 nm) can be understood based on the difference of the atom positions in the domains with opposite polarity.^{21,22,35} During polarisation reversal the G2, G3, and SO_4 molecules are only slightly shifted in their positions, whereas the NH_3 group of G1 moves 0.09 nm along the b axis. The position of the NH_3 group is either 0.045 nm above or below the plane $b/4$ (or $3b/4$, respectively) for the two different polarization directions. The positive side of the polarization vector is directed from the plane $b/4$ (or $3b/4$) to the actual position of layer A (or A').²² The cleavage plane is the positive side of these layers¹⁹ (see Fig. 6).

Figure 6(a) shows the sample right after the cleavage. On both fresh surfaces the steps at the domain boundaries have heights of $b/4 + \Delta$. After the removal of a complete monolayer with thickness $b/2$ at the positive domains of sample I the step height at the domain boundaries of this sample change to $b/4 - \Delta$. From the SFM measurements the value of Δ is estimated to be 0.05 nm, which is in good agreement with the x-ray diffraction data.³⁵

The influence of electrostatic interactions between the Si_3N_4 SFM tip and the electric field of the sample on the step heights measured in our experiment could be excluded. The applications of voltages with different polarity between tip and sample did not change the measured step heights.

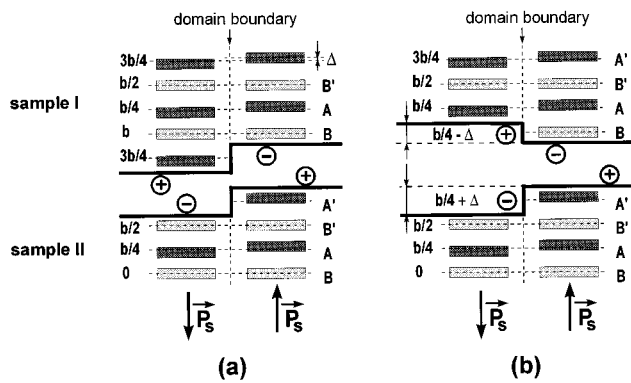


FIG. 6. Explanation of the different step heights measured at the domain boundaries of samples I and II. The arrangement of the sample is analogous to Fig. 4. The mean position of the layers B and B' remains almost unchanged for domains of opposite polarity, whereas the layers A and A' are shifted by a distance of Δ along the \mathbf{b} axis. The sign of the shift determines the direction of the polarization vector \mathbf{P}_s . (a) The sample in the moment of cleavage. The cleavage plane is the positive side of the layers A or A'. On both cleavage faces the step at the domain boundary has a height of $\mathbf{b}/4 + \Delta$. (b) On surface I a monolayer with thickness $\mathbf{b}/2$ is etched away. The remaining step at the domain boundary has a height of $\mathbf{b}/4 - \Delta$.

IV. SUMMARY

It has been shown that the etch fine structure of ferroelectric domains on opposite cleavage faces of TGS varies strongly even for domains of equal polarity. The mismatch of the cleavage faces at the domain boundaries was presumed to result from the dissolution of a complete monolayer on the positive domains on one cleavage face. The relative shifts in the atom positions during polarization reversal could be measured at the domain boundaries. The results are consistent with earlier measurements done by x-ray diffraction, TEM, and optical microscopy.

ACKNOWLEDGMENTS

The authors would like to thank K. Szczesniak from the Institute of Molecular Physics of the Polish Academy of Sciences for supplying the TGS samples. The authors also thank U. D. Schwarz and A. Wadas for helpful discussions.

- ¹B. T. Matthias, C. E. Miller, and J. R. Remeika, *Phys. Rev.* **104**, 849 (1956).
- ²V. P. Konstantinova, I. M. Silvestrova, and V. A. Yurin, *Kristallografiya* **4**, 125 (1959).
- ³N. Nakatani, *Jpn. J. Appl. Phys.* **12**, 1723 (1973).
- ⁴G. I. Distler, V. P. Konstantinova, Y. M. Gerasimov, and G. A. Tolmacheva, *Nature* **218**, 762 (1968).
- ⁵B. Hlczler, Cz. Pawlaczyk, L. Szczesniak, K.-P. Meyer, and R. Scholz, *Mater. Sci.* **7**, 427 (1981).
- ⁶N. Nakatani, *Jpn. J. Appl. Phys.* **12**, 313 (1973).
- ⁷L. Szczesniak and L. Szczepanska, *Ferroelectrics* **111**, 167 (1990).
- ⁸H. Haefke, R. Lüthi, K.-P. Meyer, and H.-J. Güntherodt, *Ferroelectrics* **151**, 143 (1994).
- ⁹N. Nakatani, *J. Phys. Soc. Jpn.* **39**, 741 (1975).
- ¹⁰N. Nakatani, *Jpn. J. Appl. Phys.* **24**, L528 (1985).
- ¹¹N. Tomita, H. Orihara, and Y. Ishibashi, *J. Phys. Soc. Jpn.* **58**, 1190 (1989).
- ¹²J. A. Hooton and W. J. Merz, *Phys. Rev.* **98**, 409 (1955).
- ¹³V. P. Konstantinova, *Kristallografiya* **7**, 748 (1962).
- ¹⁴V. A. Meleshina, *Kristallografiya* **16**, 557 (1971).
- ¹⁵F. Giletta, *Phys. Status Solidi A* **11**, 721 (1972).
- ¹⁶G. I. Distler, V. N. Lebedeva, and E. V. Krasilnikova, *Bull. Acad. Sci. USSR Phys. Ser.* **44**, 86 (1980).
- ¹⁷A. Sawada and R. Abe, *Jpn. J. Appl. Phys.* **6**, 699 (1967).
- ¹⁸H. Bluhm, U. D. Schwarz, K.-P. Meyer, and R. Wiesendanger, *Appl. Phys. A* (to be published).
- ¹⁹N. Nakatani, *Jpn. J. Appl. Phys.* **18**, 491 (1979).
- ²⁰E. A. Wood and A. N. Holden, *Acta Crystallogr.* **10**, 145 (1957).
- ²¹S. Hoshino, Y. Okaya, and R. Pepinsky, *Phys. Rev.* **115**, 323 (1959).
- ²²B. Brezina and M. Havránková, *Cryst. Res. Technol.* **20**, 781 (1985).
- ²³Digital Instruments, Santa Barbara, CA.
- ²⁴N. Nakatani, *Jpn. J. Appl. Phys.* **25**, 27 (1986).
- ²⁵R. B. Heimann, *Auflösung von Kristallen* (Springer, Berlin, 1975).
- ²⁶R. Gross and A. d. K. Sächs. Ges. Wiss. Leipzig, *Math-Phys. Kl.* **35**, 137 (1928).
- ²⁷B. Batterman, *J. Appl. Phys.* **28**, 1236 (1957).
- ²⁸E. Ernst, *Z. Kristallogr.* **63**, 153 (1926).
- ²⁹B. A. Irving, *J. Appl. Phys.* **31**, 109 (1960).
- ³⁰R. J. Jaccodine, *J. Appl. Phys.* **33**, 2643 (1962).
- ³¹J. D. Venables, *Phys. Rev.* **122**, 1388 (1961).
- ³²C. C. Desai and M. S. V. Ramana, *Cryst. Res. Technol.* **24** K173 (1989).
- ³³P. Cordier, B. Boulogne, N. Doukhan, and J. C. Doukhan, *Phys. Status Solidi A* **112**, 493 (1989).
- ³⁴V. P. Sergeev, E. A. Budovskikh, L. B. Zuev, and G. I. Gol'denberg, *Sov. Phys.-Cryst.* **31**, 361 (1986).
- ³⁵S. R. Fletcher, E. T. Keve, and A. C. Skapski, *Ferroelectrics* **14**, 775 (1976).